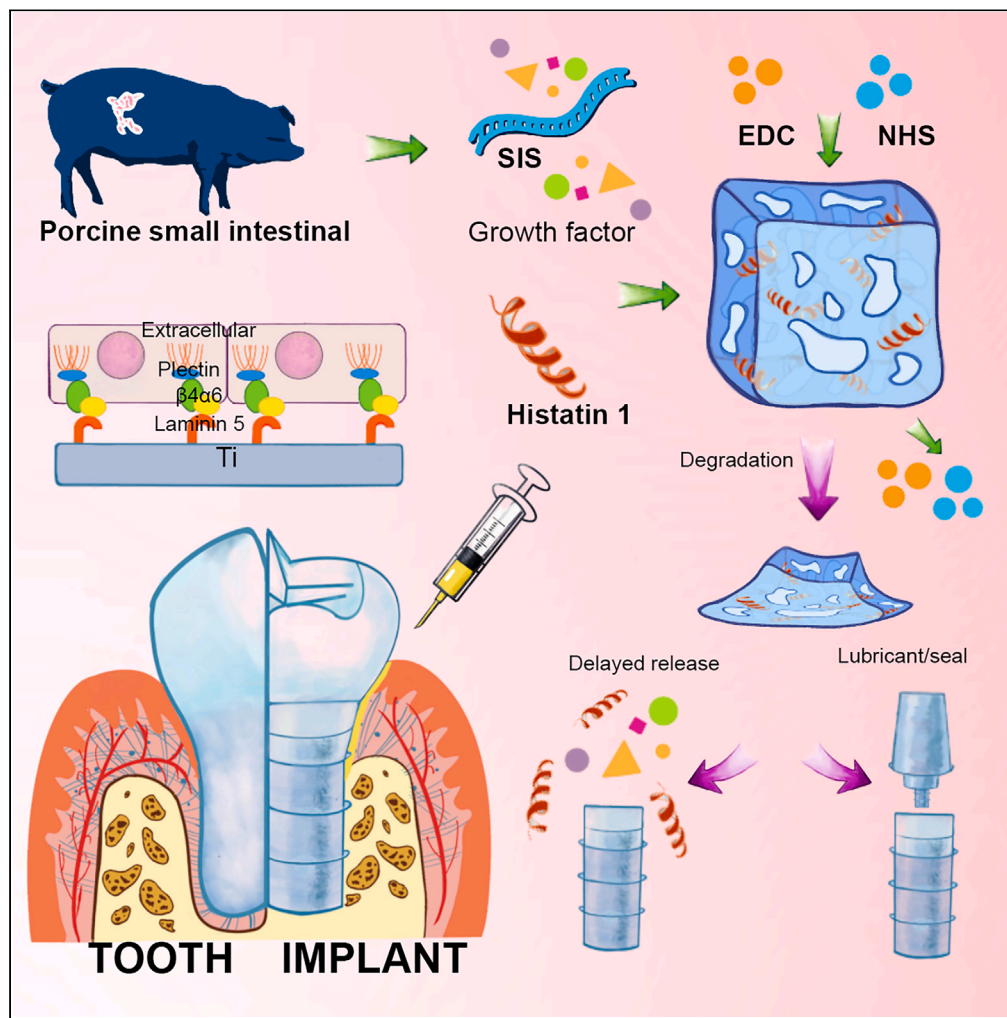


Article

Histatin 1-modified SIS hydrogels enhance the sealing of peri-implant mucosa to prevent peri-implantitis



Zihao Liu, Yaqi Du, Shendan Xu, ..., Bo Zhao, Pengfei Wei, Yonglan Wang

zhaobo@biosishealing.com (B.Z.)
weipengfei@biosishealing.com (P.W.)
tmuperiodontology@163.com (Y.W.)

Highlights

Promote cell proliferation and adhesion

Local administration around the implant

Hemidesmosomes synthesis gets improved

Satisfactory soft tissue healing and sealing



Article

Histatin 1-modified SIS hydrogels enhance the sealing of peri-implant mucosa to prevent peri-implantitis

Zihao Liu,^{2,5} Yaqi Du,^{1,5} Shendan Xu,^{1,5} Minting Li,¹ Xuemei Lu,¹ Guangjie Tian,¹ Jing Ye,³ Bo Zhao,^{4,*} Pengfei Wei,^{4,*} and Yonglan Wang^{1,6,*}

SUMMARY

Dental implants make it possible to replace teeth in more sophisticated ways. Nevertheless, peri-implantitis is one of the leading causes of implant failure, which can be avoided with proper soft tissue sealing. The aim of this study was to achieve the promotion of the synthesis of peri-implant epithelial hemidesmosome through Histatin 1 and porcine small intestinal submucosa (SIS) hydrogel to form a good peri-implant seal. The results show that hydrogel can improve the biological barrier function around implants by combining antibacterial, promoting soft tissue healing and promoting epithelial bonding. This means that the morphology and anti-infection ability of soft tissue are enhanced, which ensures the long-term stability of the implant. SIS-Hst1 hydrogel has certain clinical application in the prevention and early treatment of peri-implantitis. In conclusion, Hst1-SIS hydrogel, as a local administration system, provides experimental evidence for the prevention of peri-implant disease.

INTRODUCTION

The implant is a safe and predictable way to treat completely and partially absent teeth. One of the major factors affecting its survival rate is peri-implant disease.¹ Peri-implant diseases are inflammation of the surrounding soft and hard tissues related to bacterial infection, which often leads to implant loosening and falling out.² Therefore, it is urgent to design strategies to take precautions against peri-implant diseases. Recently, it has been proved that the soft tissue seal around the implant can effectively resist physical and pathological stimulation.^{3,4} By improving the interaction of epithelial cells with the titanium surface and enhancing the stability of the implant during healing, it is possible to avoid the growth of bacteria and their metabolites, thereby lowering the risk of inflammation and marginal bone loss.⁵⁻⁷ The prevention of peri-implant disease involves soft tissue sealing as a crucial component.

The sealing of the soft tissue surrounding healthy teeth and implants is maintained by the Junctional epithelium (JE).⁸ JE is composed of substrate and hemidesmosome (HD). The attachment of JE mainly depends on the anchoring effect of HD, and HD are highly specialized epithelial attachment structures on the substrate.⁹⁻¹¹ However, due to the ischemic state of the tissue surrounding the implant and the release of metal ions from the implant, the proliferation of peri-implant cells is slow. Only 1/3 of the attached epithelium around the implant's root forms the HD, and the number is significantly less than that around the natural teeth.^{12,13} This results in the peri-implant mucosa being less resistant than the gingiva at adjacent natural teeth sites.¹⁴

Favorable properties of peptides, such as low toxicity, intercellular communication, and involvement in host defense, make peptides an attractive approach for therapeutic drug development. Histatin1 (Hst1) is derived from human salivary glands such as the submandibular and parotid glands.¹⁵ It can potentially maintain the integrity of soft tissues by affecting the extension of epithelial cells and cell adhesion and migration.¹⁶ Studies have shown that Hst1 can promote the adhesion between cells and the surface of implanting materials (titanium, hydroxyapatite, etc.), and participate in forming the host's natural immune system.^{17,18} Van Dijk et al. systematically studied the process of Hst1 promoting the dynamic adhesion of epithelial cells on the titanium surface and speculated that this process was produced by activating integrin-mediated cell adhesion.^{19,20} As the transmembrane part of HD, integrin $\alpha\beta4$ initiates the assembly of HD, thereby mediating cell adhesion and epithelial adhesion to improve soft tissue sealing around the implant.^{21,22} There should be tremendous potential for the application of Hst1 in the soft tissue around the implant. The effects of Hst1 may be inhibited or enzymatically hydrolyzed if it is applied directly, and

¹School and Hospital of Stomatology, Tianjin Medical University, Tianjin 30070, China

²Zhongnuo Dental Hospital, Tianjin Nankai District, Tianjin 300101, China

³Department of Stomatology, Tianjin Hospital, Tianjin 300211, China

⁴Beijing Biosis Healing Biological Technology Co., Ltd., Beijing 102600, China

⁵These authors contributed equally

⁶Lead contact

*Correspondence: zhaobo@biosishealing.com (B.Z.), weipengfei@biosishealing.com (P.W.), tmuperiodontology@163.com (Y.W.)

<https://doi.org/10.1016/j.isci.2023.108212>



a shorter period between doses is also necessary. Therefore, finding a carrier material to enable prolonged release of HST1 in the tissue is indeed required in order to accomplish a suitable application.

Hydrogel is a carrier material that has been extensively used in clinics. It can simulate the complex extracellular environments, provide structural support for the defect, and deliver the therapeutic materials dissolved within the materials to the surrounding tissues.²² Among them, thermosensitive hydrogels have been widely studied in the fields of tissue pharmaceuticals and engineering because of they maintain a liquid state at low temperatures and transforming into gels at 37°C.²³ The thermosensitive hydrogel can act as a lubricant when it is liquid, decreasing the interface friction and thereby increasing the preload between the implant and the abutment.^{24,25} When it is converted into a gel state, it can seal the micro gap between the implant and the abutment, prevent the invasion of bacteria and their metabolites, and improve the stability of the abutment. The application of thermosensitive hydrogel around the implant allows for its good biocompatibility and liquid-gel phase transition properties to be exploited. Based on previous research by our group, we chose small intestinal submucosa (SIS) to prepare thermosensitive hydrogels. The main components of SIS are type I and type III collagens, which have good biocompatibility. The prepared thermosensitive hydrogels have good physical properties. In addition, SIS contains a variety of active factors such as proteoglycan, elastin, glycosaminoglycan, growth factor, etc., which can provide an integral cell growth microenvironment to promote cell proliferation.^{26–28} We believe that SIS, as a raw material for hydrogels, can be used as a carrier for the sustained release of Hst1. At the same time, it can compensate for each other through different signal pathways to promote the formation of epithelial attachment and improve the sealing of the soft tissue around the implant.

In this study, we design Hst1-modified SIS thermosensitive hydrogels. This study will explore the sealing effects of Hst1 hydrogels on the peri-implant epithelium promoted by *in vitro* cell experiments and *in vivo* experiments. This research aims to adopt this kind of hydrogel to enhance the biological closure around the implant and provide a new method for preventing peri-implant diseases.

RESULT AND DISCUSSION

Preparation and characterization of hydrogels

The hydrogel was synthesized by the aforementioned method, and after lyophilization, we could see the loose and porous structure formed and the loading of peptides by scanning electron microscopy (Figure 1A). Cross-linking brings small through-pore structures around large pores, increasing the porosity of the structure, which not only provides more cell adhesion sites but also facilitates the co-supply of nutrients and the discharge of metabolites.^{29,30}

Certain mechanical properties are provided by the hydrogel's structure. The hydrogel has a certain fluidity before gelation and changes its shape through temperature changes to adapt to the shape of the tissue. SIS was transformed into a gel at 37°C (Figures 1Ba and 1Bb), and the mechanical properties were examined by compressive tests (Figure 1C) and rheological tests (Figures 1F, 1G, and S1–S4). The stress-strain relationship was studied with a compressive testing machine; when the strain is 79%, the tensile strength of the hydrogel can reach 81 kPa. At 37°C, its storage modulus is greater than the loss modulus, and the material is in a semi-solid mode. The elastic modulus value of Hst1 has little change. It demonstrates that the addition of Hst1 does not affect the mechanical properties of the hydrogel.³¹

In the process of hydrogel synthesis, the stable combination of Hst1 and SIS hydrogel is required for the sustained release of Hst1. Considering its application, the chemical cross-linking method is a cheaper and simpler preparation methods. However, most of the chemical cross-linking agents are toxic to the human body, so the low-toxicity cross-linking agent is still an important factor to be considered. 1-Ethyl-3-(3-dimethyl aminopropyl) carbodiimide (EDC) is a water-soluble, non-cytotoxic chemical cross-linking agent that can stably cross-link amino groups as a coupling agent. N-hydroxy succinimide (NHS) is used as a stabilizer to increase cross-linking efficiency.^{32,33} EDC and NHS activate the carboxyl group of the collagen and form an amide bond with the amino group of the polypeptide.³⁴ After the reaction, the cross-linking agent (Scheme 1A) can be removed by dialysis.³⁵

After cross-linking, we verified the release of Hst1 in the hydrogel, and it was visually seen that the color of the fluorescent Hst1-labeled hydrogel faded with the release of Hst1 (Figures 1Bc and 1Bd). At the same time, the release was quantitatively analyzed by measuring the absorbance of the labeled fluorescent peptide (Figures 1C and S5). The results of sustained release showed that Hst1 without cross-linking was completely released after 2 days, while after cross-linking it could be released for about 1 week. There was little difference between HST1 and HST1 without cross-linking in the second week. In addition, there was no statistical difference in the effect of Hst1 concentration on sustained release. We verified the swelling property of hydrogel (Figure 1D). The swelling reached equilibrium in about 400 min; the swelling rate of cross-linked hydrogel was relatively low. This is related to the cross-linking effect of EDC and NHS on collagen, which makes the relative structure of gel more stable. Regarding the degradation of hydrogel (Figure 1E), the degradation curve of hydrogel is basically proportional to time. We speculate that Hst1 is released as the SIS hydrogel diffuses or degrades, and the amide bond is broken, thereby being released into surrounding tissues. Based on the aforementioned results, SIS-Hst1 hydrogel has thermosensitivity and certain mechanical strength and can be sustained release after cross-linking, so it has a great application prospect in injection.

Cell biocompatibility

Cell live/dead staining (Figure 2A) analysis was used to evaluate the cytotoxicity of the material, within the field of view of the blank group, SIS group. However, SIS-Hst1(L) group and SIS-Hst1(H) group after coculture for 12/24 h showed almost no dead cells. At the same time, the number of cells in the field was counted. It could be seen that there was a statistical difference in the number of cells relative to the blank group, but there was no significant statistical difference in the cell appreciation of the hydrogel group. The Cell counting Kit-8 (CCK-8)

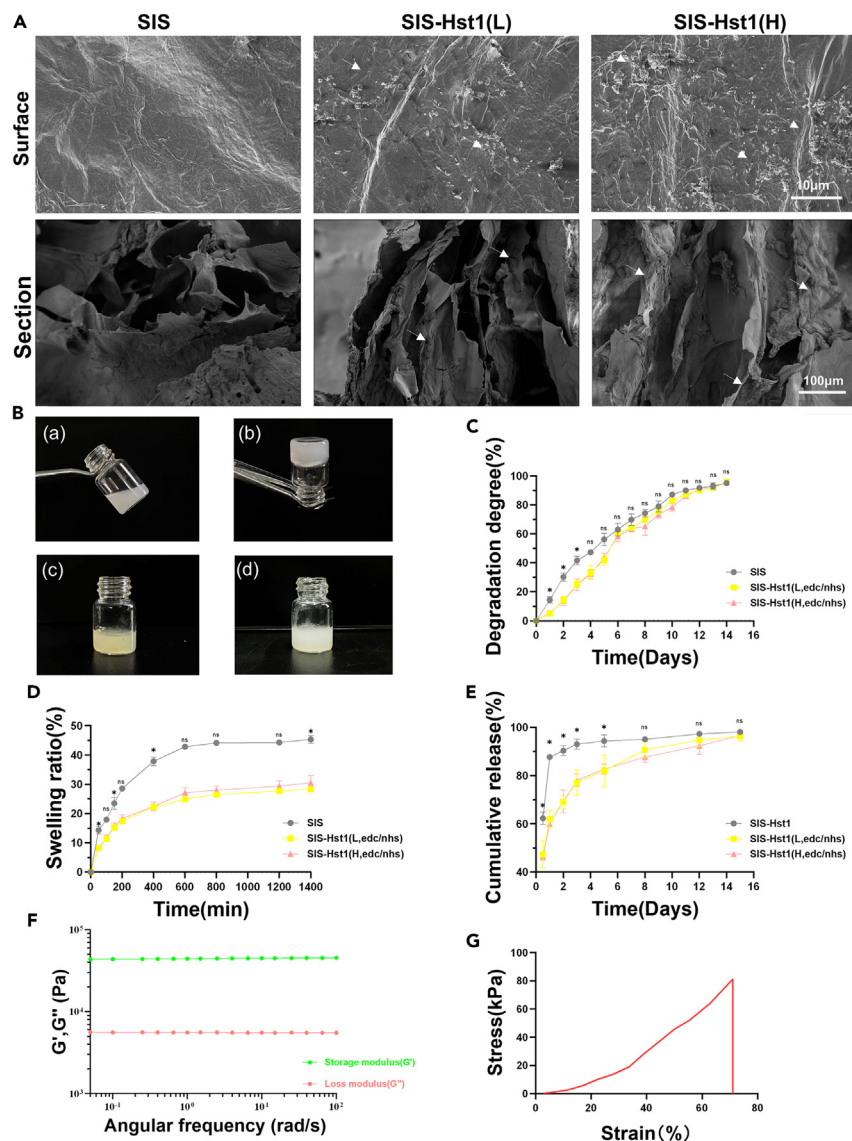


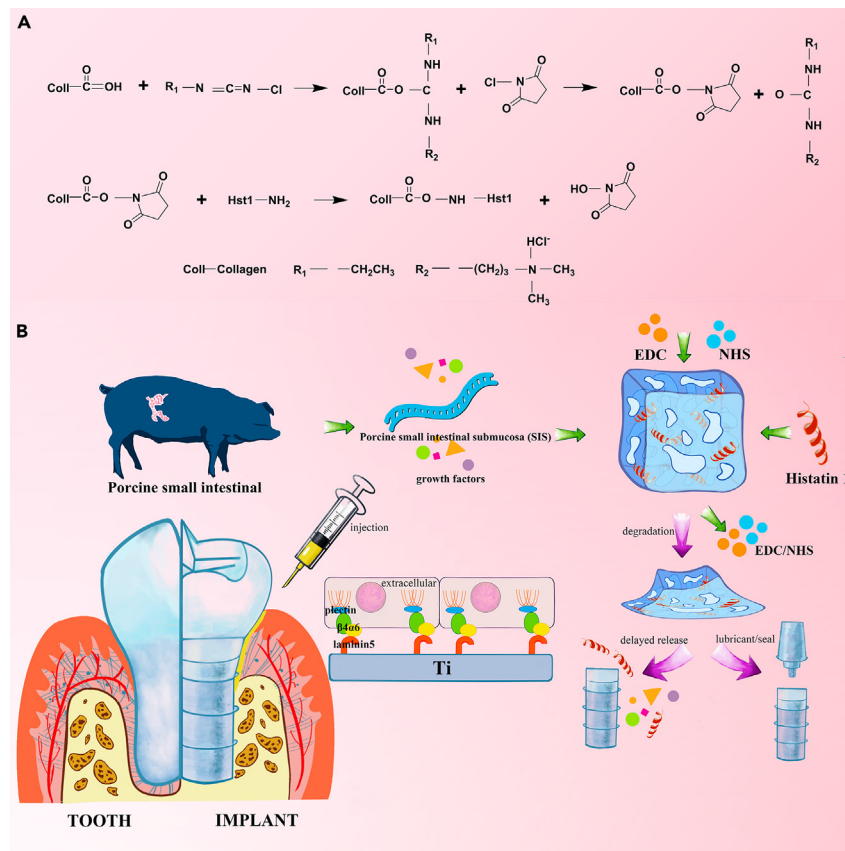
Figure 1. Preparation and characterization of hydrogels

(A) Surface and cross-section of hydrogel under SEM. The arrow shows the Hst1; (B) Visual photographs (a) Hydrogel at room temperature (b) Hydrogel at 37°C (c) Fluorescent Hst1 labeling (d) Hydrogel after release for 2 weeks; (C) The release profile of Hst1 in hydrogel; (D) Swelling ratio of hydrogel; (E) Degradation rate of hydrogel; (F) Storage modulus (G') and loss modulus (G'') of the Hst1-SIS(H) hydrogel under strain amplitude sweep (γ 0.1%–1000%) at a fixed angular frequency; (G) Hst1-SIS(H) Stress-Strain curve.

cell count analysis was used to evaluate cell proliferation within 7 days (Figure 2B). The proliferation of other cells was enhanced compared with the blank group, but there was no statistical difference in cell proliferation between the SIS-Hst1 group and the SIS hydrogel group.

The immunohistochemical study around the implant confirmed that the cell proliferation and regeneration ability of the peri-implant epithelium were weaker than those of the JE.³⁶ Therefore, it is of great significance for materials to promote cell proliferation.³⁷ The positive stimulating effect of SIS on cell proliferation, which may be related to the growth factors preserved by SIS, including transforming growth factor β , basic fibroblast growth factor (FGF), hepatocyte growth factor, and vascular endothelial growth factor (VEGF), is retained in the extracellular matrix biological scaffold in their bioactive form after sterilization.^{38–40} These growth factors and collagen, proteins, and other components enhance cell adhesion and activate signals to affect cell differentiation and regeneration potential. Compared with the control group containing only SIS hydrogel, the effect of Hst1 introduction on cell proliferation was not statistically different, which is consistent with the previous research results.

S. gordonii is an early colonization bacterium of peri-implantitis. The antibacterial activity of *S. gordonii* was tested. The results revealed that all the extracts in the hydrogel group had certain antibacterial effect. The antibacterial region (Figure 2C) of SIS-HST1 was slightly larger



Scheme 1. Schematic diagram of the application of Hst1-SIS hydrogels

(A) EDC/NHS chemical cross-linking agent; (B) Shows the synthesis of hydrogels and potential applications of hydrogels around implants.

than that in the SIS group, but there was no significant statistical difference. The staining results for colony forming units count agar plates (Figure 2D) and live/dead bacteria (Figure 2E) were similar, and the hydrogel groups all displayed antibacterial activity. We speculated that Hst1 might have a certain synergistic effect, but the effect was subtle. Above all, the results demonstrated that the hydrogel is biocompatible.

Cell adhesion and migration

Transwell's experiment (Figure 3A) revealed that the hydrogel promoted cell migration. By counting and observing, compared with other groups, SIS-Hst1(H) will have a stronger effect on cell migration. Cell migration ability is an essential part of wound healing.⁴¹ Previous studies have found that Hst1 promotes the effective healing of oral wounds by activating the 2 (RIN2)/Rab5/Rac1 signaling pathway to enhance cell migration, which may relate to the vascular endothelial growth factor receptor.⁴² The promotion of cell migration on tissue and titanium by Hst1 is beneficial to tissue regeneration and to the subsequent adhesion of cells on titanium.

Cells were cultured on titanium sheets containing hydrogel and observed under scanning electron microscope (SEM) (Figure 3B). Compared with the blank group, the appearance of cell pseudopodia was significantly observed in the SIS hydrogel group. It shows that the SIS hydrogel has a certain promoting effect on cell adhesion. As a hydrogel whose main component is collagen, SIS can effectively improve cell affinity and promote early cell adhesion and extension. On the other hand, cells on the surface of SIS-Hst1 hydrogel showed more obvious lamellipodia and filopodia, showing stronger cell biological activity. This indicates that Hst1 can promote the extension of cell pseudopodia. We think this as the dynamic changes of cell surface expansion, and the early changes of cell migration prove that Hst1 also has a certain influence on cell movement.⁴³ The adhesion of cells in the SIS-Hst1 hydrogel group was superior to that in the SIS hydrogel group, which confirmed the synergistic effect of the two materials. The cytoskeletal morphology (Figure 3C) was consistent with the SEM data.

Hydrogel promotes the synthesis of HD

(IF) detected the expressions of HD-related proteins laminin 5, integrin- $\alpha 6$, and integrin- $\beta 4$ in human gingival epithelial cells (hGECs). Among these proteins, laminin 5 is mainly distributed in the cytoplasm, and integrin- $\alpha 6$ is mainly distributed on the surface of the cell membrane (Figure 4). By IF staining, the laminin 5, integrin- $\alpha 6$, integrin- $\beta 4$ proteins widely distributed in the cells could be observed in the SIS-Hst1 group,

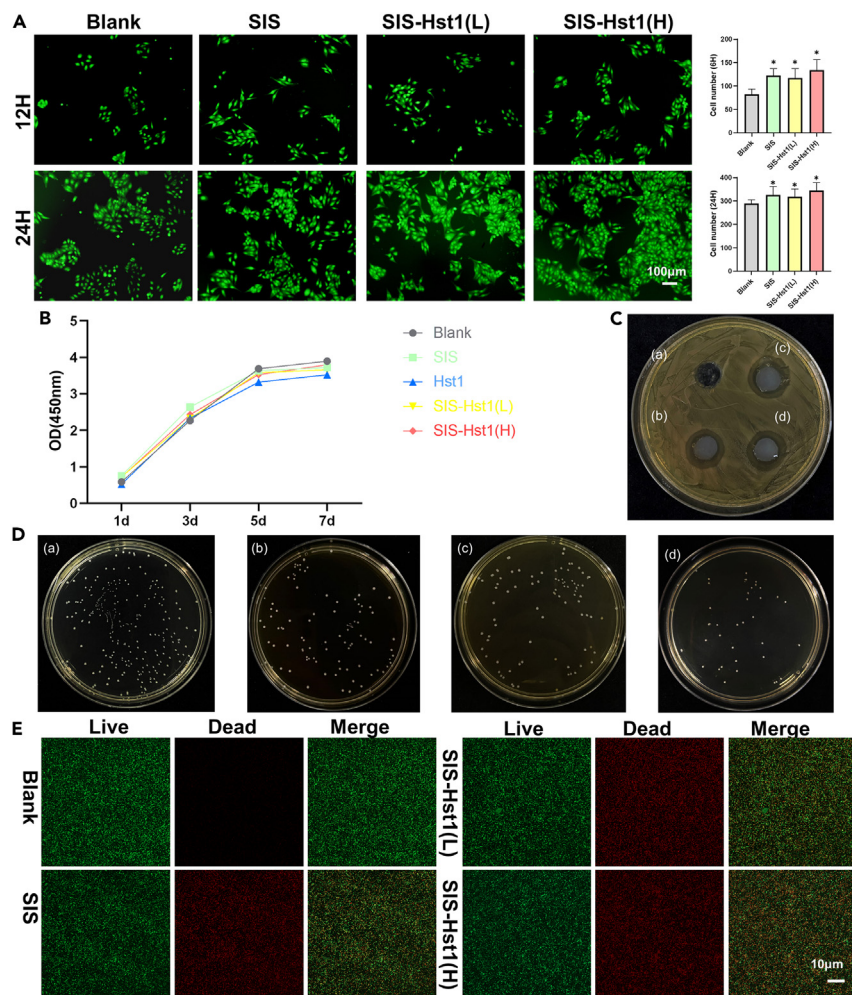


Figure 2. Cell biocompatibility

(A) Cell live/dead staining of cells cultured at 12h and 24h. At the right is the corresponding living cell count.

(B) CCK-8 detection of cell proliferation; (C) Inhibition zones of *S. gordonii* co-cultured (a) Blank (b) SIS (c) SIS-Hst1(L) (d) SIS-Hst1(H); (D) Photographs of colony forming units count agar plates (a) Blank (b) SIS (c) SIS-Hst1(L) (d) SIS-Hst1(H). At the right is the corresponding relative bacterial numbers; (E) Fluorescent LIVE/DEAD staining images of *S. gordonii*.

and they were stronger than those in the blank group. It shows that SIS-Hst1 hydrogel can effectively promote the expression of laminin 5, integrin- $\alpha 6$, and integrin- $\beta 4$ in hGECs. Western blot (Figures 5A and 5B) results also demonstrated this. Therefore, the expression of laminin 5, integrin- $\alpha 6$, and integrin- $\beta 4$ in hGECs was detected. The expressions of laminin 5, integrin- $\alpha 6$, and integrin- $\beta 4$ in SIS-Hst1 group were higher than those in the blank group, while the expression of SIS-Hst1(H) was the best. qRT-PCR results showed that the mRNA expression levels of laminin 5, integrin- $\alpha 6$, and integrin- $\beta 4$ were the lowest in the blank group and the highest in the SIS-Hst1(H) group (Figure 5C). The results indicated that SIS-Hst1 hydrogel could promote the expression of HD-related factors. Integrin $\alpha 6 \beta 4$ is the critical component of transmembrane HD, with intermediate plectin connecting the basal layer and the underlying structure of keratinocytes, which is the main adhesion structure. It regulates laminin 5. The ligand (LG) domain of laminin 5 interacts with integrin $\alpha 6 \beta 4$, and the basal keratinocytes will adhere to the internal basal lamina (IBL) connecting enamel through this structure.⁴⁴ The expression level of integrin protein in hGECs is upregulated, which proves that the cell adhesion ability is enhanced. Integrin $\alpha 6 \beta 4$ not only supports the adhesion of basal keratinocytes but also maintains cell proliferation. At the same time, the composite signal of integrin and growth factor activates focal adhesion kinase (FAK), and its function is related to wound healing, including the formation, migration, proliferation, survival, and expression of polarized lamellipodia.⁴⁵ This is also consistent with the aforementioned experimental results.

In vivo experiments

According to the results of *in vitro* experiments, SIS-Hst1(H) was generally superior to SIS-Hst1(L) in the selection of experimental concentrations, so we directly selected SIS-Hst1(H) as the experimental group for *in vitro* experiments. And we choose the peri-implant epithelium

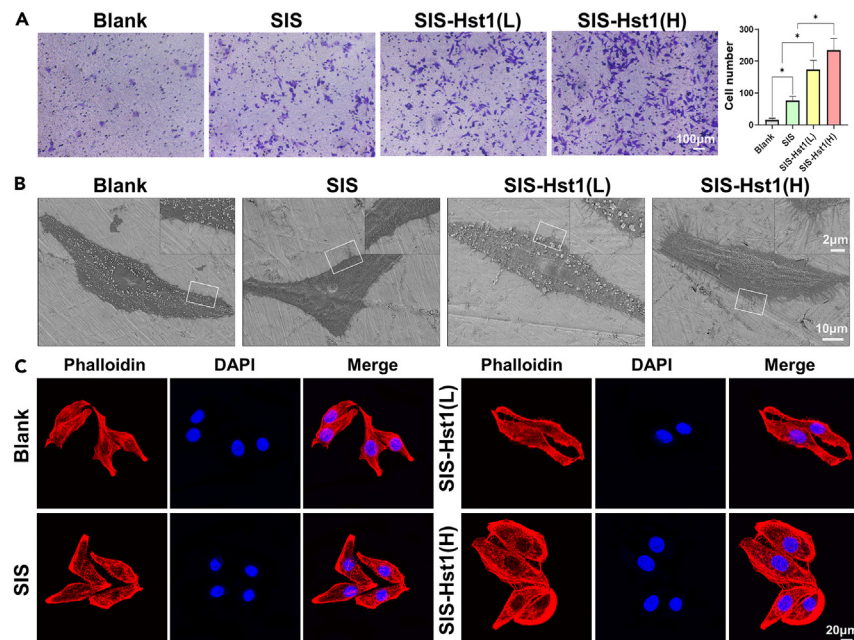


Figure 3. Cell adhesion and migration

(A) Transwell detection of cell migration ability. At the right is the corresponding of migrated cells count; (B) Observing the cell morphology under SEM, and the illustration shows a higher magnification image in a white frame; (C) Cytoskeleton staining.

of the simple implant group (smooth) as the control group. If the peri-implant epithelium around the implant is not well combined with the implant, inflammation will quickly affect the surrounding tissues including the underlying bone tissue.⁴⁶ At the same time, the mucosa will be painful and discolored, which is double harm to the function and aesthetics after implantation. The peri-implant epithelium is more like the JE of natural teeth in all aspects; the closer it is combined with implants, the stronger its ability to resist external toxic substances and the better its soft tissue sealing ability.⁴⁷ So at the same time, the epithelial tissue of rat tooth was also taken as the contrast of normal tissue. After the first molar was extracted and the implant was implanted, the morphology of the JE and peri-implant epithelium of the rats were preliminarily observed (Figure 6A). The epithelial regeneration was observed 1 week after the operation, and it could be seen that a thin epithelial layer had been formed around the implants in each group. The histological morphology of SIS-Hst1 group was closer to natural teeth. The JE of natural teeth is a stratified squamous non-keratinizing epithelium consisting only of the stratum basale and the stratum suprabasale.⁴⁸ Basal cells face the gingival connective tissue. The basal cells and the adjacent suprabasal cell layer are cuboidal to slightly spindle-shaped. The basal cell layer of SIS-Hst1 consists of 3–5 layers of flat cells, which are more than those of SIS and blank groups, and the morphology is similar to that of the JE. All remaining cells in the suprabasal layer are flat and parallel to the tooth surface and are very similar to each other. While the suprabasal layer cells in the smooth group are not flat enough, and the nuclei are obvious, it may be due to certain inflammatory infiltration. Inflammatory infiltration often affects the initial stability of implants.⁴⁹ Antibiotics can reduce inflammatory infiltration and accelerate epithelization.⁵⁰ However, the morphology of basal upper layer cells in SIS group and SIS-Hst1 group is better than that in smooth group, which is related to the antibacterial activity of SIS components. In general, the supra-basal layer cells of SIS-Hst1 are the closest to natural teeth. In overall morphology, both SIS-Hst1 and JE tapered in the apical direction.⁵¹ Combined with the results *in vitro*, SIS-Hst1 hydrogel has the functions of promoting healing and epithelial bonding, and at the same time, it can reduce inflammatory infiltration and play a synergistic role in healing, so that the rat peri-implant epithelium treated with SIS-Hst1 hydrogel has the shape closest to natural teeth.

The expression and distribution of HD-related proteins at the implant interface were detected by IF staining (Figure 6B). HD is critical for epithelial attachment stabilization. Laminin 5 is an extracellular component of HD, and integrin $\alpha 6 \beta 4$ is mainly a transmembrane protein.⁵² The formation of HD can be inferred by measuring the expression of these main proteins. One week later, the expression of laminin 5 could be detected in both the basal layer and the suprabasal layer around the implant; especially the expression of SIS-Hst1 in the inner and outer layers of the peri-implant epithelium was significant. Laminin 5 plays a role in guiding epithelial healing, and its higher expression also represents increased epithelial migration and re-epithelialization. SIS-Hst1 basically has a fluorescent band appearing. The expression of integrin- $\alpha 6$ is more evident in the middle part, and the expression of integrin- $\beta 4$ is more obvious in the middle and lower parts. Overall, it can be seen that the protein expression level of SIS-Hst1 is relatively high. Therefore, we speculate that SIS-Hst1 hydrogel can promote the formation of HD around implants. In conclusion, the peri-implant epithelium formed after the hydration treatment of SIS-Hst1 is closer to the natural teeth and increases the synthesis of the key anchoring factor HD, which can effectively improve the soft tissue

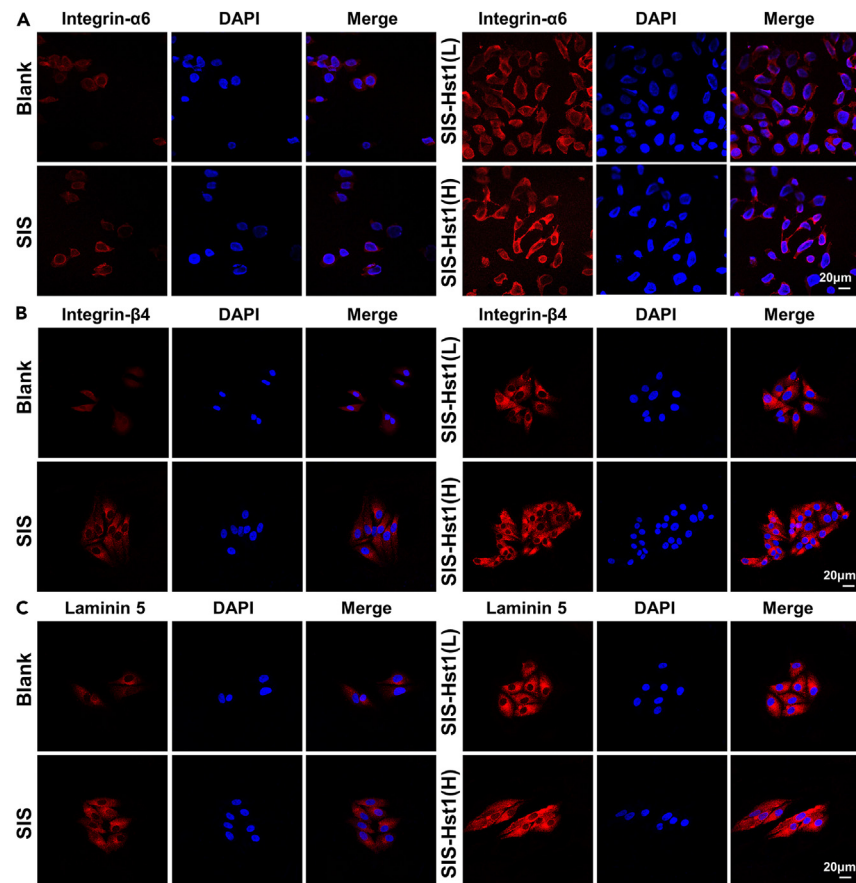


Figure 4. Immunofluorescence staining

Immunofluorescence analysis of Integrin- $\alpha 6$ (A), Integrin- $\beta 4$ (B), laminin 5 (C), related protein localization. (Red is the protein, blue is the nucleus and the result of the synthesis).

closure around the implant. It is possible to prevent peri-implantitis and provide possible therapeutic prospects for early adjuvant treatment of peri-implantitis.

Limitations of the study

The limitation of this study is that the selection of animal models is not perfect. There are two options for tooth extraction: immediate extraction and delayed extraction and implantation. For research purposes, we only opted for immediate tooth extraction and implantation.

The main difference between the two models is that the healing results at the bone level are different. Because this study focuses on the horizontal healing of implant soft tissue, only one of them is chosen for modeling. We think that this will have no significant impact on the results.

We hope that more animal models can be chosen to validate the results in subsequent research, thereby minimizing the experiment's limitations.

STAR★METHODS

Detailed methods are provided in the online version of this paper and include the following:

- [KEY RESOURCES TABLE](#)
- [RESOURCE AVAILABILITY](#)
 - Lead contact
 - Materials availability
 - Data and code availability
- [EXPERIMENTAL MODEL AND SUBJECT DETAILS](#)
 - Cell lines

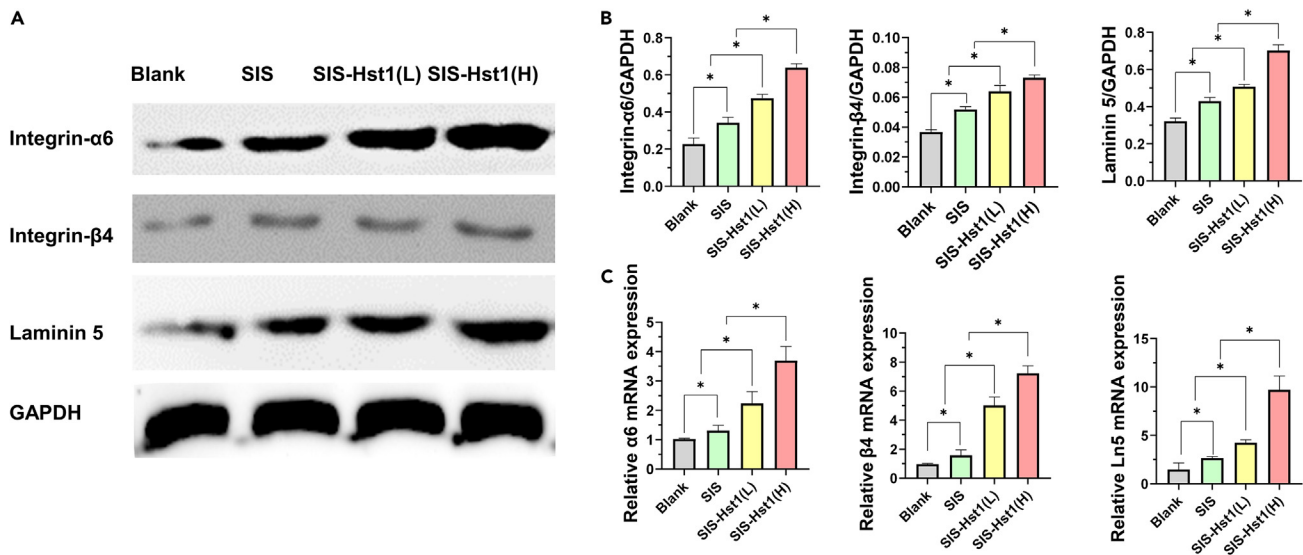


Figure 5. Western blot and qRT-PCR analysis of HD
(A) Western blot analysis of HD-related proteins; (B) Quantitative analysis of HD-related proteins; (C) qRT-PCR analysis of related genes.

● METHOD DETAILS

- Preparation of hydrogels
- Characterizations
- Antioxidant experiment
- Antibacterial test
- Cell adhesion and migration
- Real-time quantitative polymerase chain reaction (qRT-PCR)
- Western blot
- Immunofluorescence staining
- Animal experiments *in vitro*

● QUANTIFICATION AND STATISTICAL ANALYSIS

SUPPLEMENTAL INFORMATION

Supplemental information can be found online at <https://doi.org/10.1016/j.isci.2023.108212>.

ACKNOWLEDGMENTS

Z.L. and Y.D. and S.X. contributed equally to this work. Scientific Foundation of the Second Hospital of Tianjin Medical University (Grant No.2022ydey06); the Science and technology project of Tianjin Health Committee (Grant No.TJWJ2022QN054).

AUTHOR CONTRIBUTIONS

Zihao Liu: Conceptualization, Validation, Investigation, Data curation, Visualization, Supervision. Yaqi Du: Methodology, Validation, Investigation, Visualization, Formal analysis, Writing – original draft, Writing – review & editing. Shendan Xu: Validation, Formal analysis, Data curation, Visualization, Investigation. Xuemei Lu: Investigation, Visualization. Minting Li: Visualization. Guangjie Tian: Visualization. Yonglan Wang: Resources, Project administration.

DECLARATION OF INTERESTS

The authors declare no competing interests.

Received: May 27, 2023

Revised: September 15, 2023

Accepted: October 11, 2023

Published: October 14, 2023

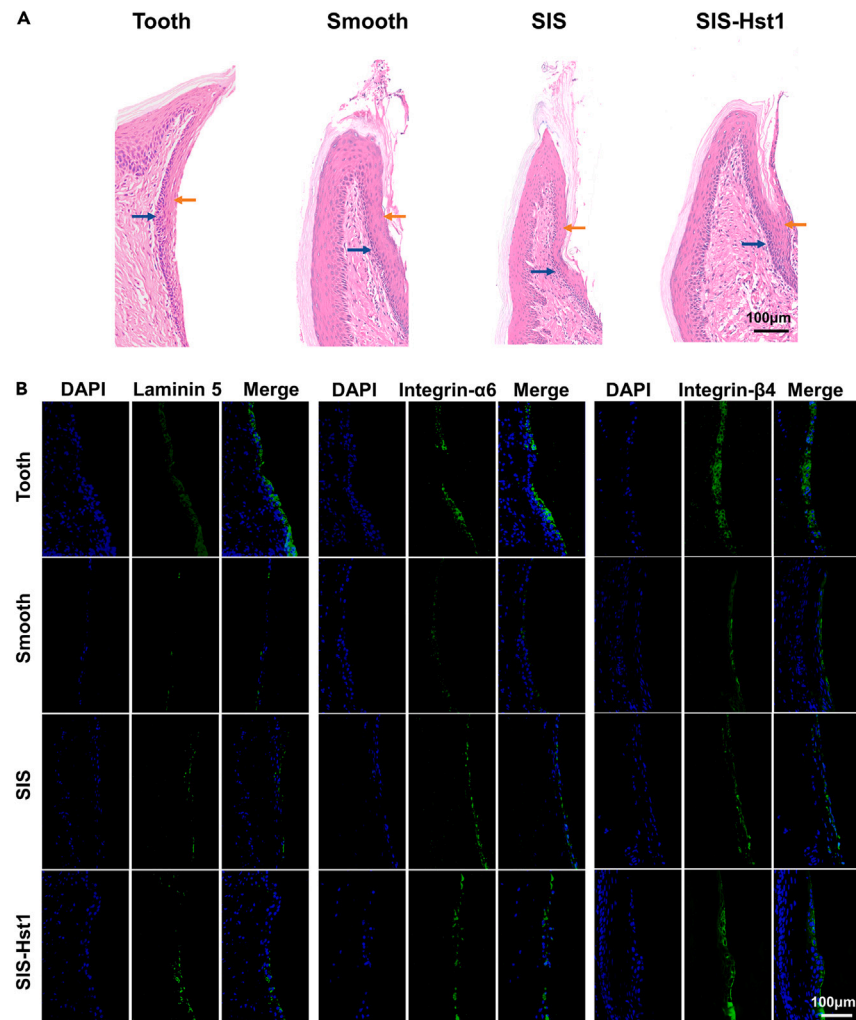


Figure 6. The results *in vivo* experiments

(A) Observation of the formation of peri-implant epithelium after HE staining. (Blue is the basal layer cell, and orange is suprabasal layer cell) (B) Immunofluorescence staining detection of protein expression and distribution. (Green is the protein, blue is the nucleus and the result of synthesis).

REFERENCES

- Elani, H.W., Starr, J.R., Da Silva, J.D., and Gallucci, G.O. (2018). Trends in Dental Implant Use in the U.S., 1999-2016, and Projections to 2026. *J. Dent. Res.* 97, 1424–1430. <https://doi.org/10.1177/0022034518792567>.
- Berglundh, T., Armitage, G., Araujo, M.G., Avila-Ortiz, G., Blanco, J., Camargo, P.M., Chen, S., Cochran, D., Derks, J., Figuero, E., et al. (2018). Peri-implant diseases and conditions: Consensus report of workgroup 4 of the 2017 World Workshop on the Classification of Periodontal and Peri-Implant Diseases and Conditions. *J. Clin. Periodontol.* 45 (Suppl 20), S286–s291. <https://doi.org/10.1111/jcpe.12957>.
- Ivanovski, S., and Lee, R. (2018). Comparison of peri-implant and periodontal marginal soft tissues in health and disease. *Periodontol* 2000 76, 116–130. <https://doi.org/10.1111/prd.12150>.
- Wang, S.S., Tang, Y.L., Pang, X., Zheng, M., Tang, Y.J., and Liang, X.H. (2019). The maintenance of an oral epithelial barrier. *Life Sci.* 227, 129–136. <https://doi.org/10.1016/j.lfs.2019.04.029>.
- Guo, T., Gulati, K., Arora, H., Han, P., Fournier, B., and Ivanovski, S. (2021). Orchestrating soft tissue integration at the transmucosal region of titanium implants. *Acta Biomater.* 124, 33–49. <https://doi.org/10.1016/j.actbio.2021.01.001>.
- Guo, T., Gulati, K., Arora, H., Han, P., Fournier, B., and Ivanovski, S. (2021). Race to invade: Understanding soft tissue integration at the transmucosal region of titanium dental implants. *Dent. Mater.* 37, 816–831. <https://doi.org/10.1016/j.dental.2021.02.005>.
- Ren, X., van der Mei, H.C., Ren, Y., and Busscher, H.J. (2019). Keratinocytes protect soft-tissue integration of dental implant materials against bacterial challenges in a 3D-tissue infection model. *Acta Biomater.* 96, 237–246. <https://doi.org/10.1016/j.actbio.2019.07.015>.
- Bosshardt, D.D., and Lang, N.P. (2005). The junctional epithelium: from health to disease. *J. Dent. Res.* 84, 9–20. <https://doi.org/10.1177/154405910508400102>.
- Shimono, M., Ishikawa, T., Enokiya, Y., Muramatsu, T., Matsuzaka, K.i., Inoue, T., Abiko, Y., Yamaza, T., Kido, M.A., Tanaka, T., and Hashimoto, S. (2003). Biological characteristics of the junctional epithelium. *J. Electron. Microsc.* 52, 627–639. <https://doi.org/10.1093/jmicro/52.6.627>.
- Tanaka, K., Tanaka, J., Aizawa, R., Kato-Tanaka, M., Ueno, H., Mishima, K., and Yamamoto, M. (2021). Structure of junctional epithelium is maintained by cell populations supplied from multiple stem cells. *Sci. Rep.* 11, 18860. <https://doi.org/10.1038/s41598-021-98398-7>.
- Yuan, X., Chen, J., Grauer, J.A., Xu, Q., Van Brunt, L.A., and Helms, J.A. (2021). The

- Junctional Epithelium Is Maintained by a Stem Cell Population. *J. Dent. Res.* 100, 209–216. <https://doi.org/10.1177/0022034520960125>.
12. Fujiseki, M., Matsuzaka, K., Yoshinari, M., Shimono, M., and Inoue, T. (2003). An experimental study on the features of peri-implant epithelium: immunohistochemical and electron-microscopic observations. *Bull. Tokyo Dent. Coll.* 44, 185–199. <https://doi.org/10.2209/tdcpub.44.185>.
 13. Zheng, Z., Ao, X., Xie, P., Jiang, F., and Chen, W. (2021). The biological width around implant. *J. Prosthodont.* Res. 65, 11–18. https://doi.org/10.2186/jpr.JPOR_2019_356.
 14. Gibbs, S., Roffel, S., Meyer, M., and Gasser, A. (2019). Biology of soft tissue repair: gingival epithelium in wound healing and attachment to the tooth and abutment surface. *Eur. Cell. Mater.* 38, 63–78. <https://doi.org/10.22203/eCM.v038a06>.
 15. Torres, P., Castro, M., Reyes, M., and Torres, V.A. (2018). Histatins, wound healing, and cell migration. *Oral Dis.* 24, 1150–1160. <https://doi.org/10.1111/odi.12816>.
 16. Pan, L., Zhang, X., and Gao, Q. (2021). Effects and mechanisms of histatins as novel skin wound-healing agents. *J. Tissue Viability* 30, 190–195. <https://doi.org/10.1016/j.jtv.2021.01.005>.
 17. Sun, W., Ma, D., Bolscher, J.G.M., Nazmi, K., Veerman, E.C.I., Bikker, F.J., Sun, P., Lin, H., and Wu, G. (2020). Human Salivary Histatin-1 Promotes Osteogenic Cell Spreading on Both Bio-Inert Substrates and Titanium SLA Surfaces. *Front. Bioeng. Biotechnol.* 8, 584410. <https://doi.org/10.3389/fbioe.2020.584410>.
 18. van Dijk, I.A., Beker, A.F., Jellema, W., Nazmi, K., Wu, G., Wismeljer, D., Krawczyk, P.M., Bolscher, J.G.M., Veerman, E.C.I., and Stap, J. (2017). Histatin 1 Enhances Cell Adhesion to Titanium in an Implant Integration Model. *J. Dent. Res.* 96, 430–436. <https://doi.org/10.1177/0022034516681761>.
 19. van Dijk, I.A., Nazmi, K., Bolscher, J.G.M., Veerman, E.C.I., and Stap, J. (2015). Histatin-1, a histidine-rich peptide in human saliva, promotes cell-substrate and cell-cell adhesion. *FASEB J.* 29, 3124–3132. <https://doi.org/10.1096/fj.14-266825>.
 20. van Dijk, I.A., Veerman, E.C.I., Reits, E.A.J., Bolscher, J.G.M., and Stap, J. (2018). Salivary peptide histatin 1 mediated cell adhesion: a possible role in mesenchymal-epithelial transition and in pathologies. *Biol. Chem.* 399, 1409–1419. <https://doi.org/10.1515/hsz-2018-0246>.
 21. Te Molder, L., de Pereda, J.M., and Sonnenberg, A. (2021). Regulation of hemidesmosome dynamics and cell signaling by integrin $\alpha 6 \beta 4$. *J. Cell Sci.* 134, jcs259004. <https://doi.org/10.1242/jcs.259004>.
 22. Wang, W., Zuidema, A., Te Molder, L., Nahidiazar, L., Hoekman, L., Schmidt, T., Coppola, S., and Sonnenberg, A. (2020). Hemidesmosomes modulate force generation via focal adhesions. *J. Cell Biol.* 219, e201904137. <https://doi.org/10.1083/jcb.201904137>.
 23. Li, Z., and Guan, J. (2011). Thermosensitive hydrogels for drug delivery. *Expert Opin. Drug Deliv.* 8, 991–1007. <https://doi.org/10.1517/17425247.2011.581656>.
 24. Fan, R., Cheng, Y., Wang, R., Zhang, T., Zhang, H., Li, J., Song, S., and Zheng, A. (2022). Thermosensitive Hydrogels and Advances in Their Application in Disease Therapy. *Polymers (Basel)* 14, 2379. <https://doi.org/10.3390/polym14122379>.
 25. Gong, C., Qi, T., Wei, X., Qu, Y., Wu, Q., Luo, F., and Qian, Z. (2013). Thermosensitive polymeric hydrogels as drug delivery systems. *Curr. Med. Chem.* 20, 79–94.
 26. Cao, G., Huang, Y., Li, K., Fan, Y., Xie, H., and Li, X. (2019). Small intestinal submucosa: superiority, limitations and solutions, and its potential to address bottlenecks in tissue repair. *J. Mater. Chem. B* 7, 5038–5055. <https://doi.org/10.1039/c9tb00530g>.
 27. Fujii, M., and Tanaka, R. (2022). Porcine Small Intestinal Submucosa Alters the Biochemical Properties of Wound Healing: A Narrative Review. *Biomedicines* 10, 2213. <https://doi.org/10.3390/biomedicines10092213>.
 28. Zhao, P., Li, X., Fang, Q., Wang, F., Ao, Q., Wang, X., Tian, X., Tong, H., Bai, S., and Fan, J. (2020). Surface modification of small intestine submucosa in tissue engineering. *Regen. Biomater.* 7, 339–348. <https://doi.org/10.1093/rb/rbaa014>.
 29. Chen, Y., Chen, Y., Xiong, X., Cui, R., Zhang, G., Wang, C., Xiao, D., Qu, S., and Weng, J. (2022). Hybridizing gellan/alginate and thixotropic magnesium phosphate-based hydrogel scaffolds for enhanced osteochondral repair. *Mater. Today. Bio* 14, 100261. <https://doi.org/10.1016/j.mtbio.2022.100261>.
 30. Wake, M.C., Patrick, C.W., Jr., and Mikos, A.G. (1994). Pore morphology effects on the fibrovascular tissue growth in porous polymer substrates. *Cell Transplant.* 3, 339–343. <https://doi.org/10.1177/096368979400300411>.
 31. Pugliese, R., and Gelain, F. (2020). Cross-Linked Self-Assembling Peptides and Their Post-Assembly Functionalization via One-Pot and In Situ Gelation System. *Int. J. Mol. Sci.* 21, 4261. <https://doi.org/10.3390/ijms21124261>.
 32. Ahn, J.I., Kuffova, L., Merrett, K., Mitra, D., Forrester, J.V., Li, F., and Griffith, M. (2013). Crosslinked collagen hydrogels as corneal implants: effects of sterically bulky vs. non-bulky carbodiimides as crosslinkers. *Acta Biomater.* 9, 7796–7805. <https://doi.org/10.1016/j.actbio.2013.04.014>.
 33. Scheffel, D.L.S., Bianchi, L., Soares, D.G., Basso, F.G., Sabatini, C., de Souza Costa, C.A., Pashley, D.H., and Hebling, J. (2015). Transdental cytotoxicity of carbodiimide (EDC) and glutaraldehyde on odontoblast-like cells. *Oper. Dent.* 40, 44–54. <https://doi.org/10.2341/13-338-l>.
 34. Adamiak, K., and Sionkowska, A. (2020). Current methods of collagen cross-linking: Review. *Int. J. Biol. Macromol.* 161, 550–560. <https://doi.org/10.1016/j.ijbiomac.2020.06.075>.
 35. Yue, T.W., Chien, W.C., Tseng, S.J., and Tang, S.C. (2007). EDC/NHS-mediated heparinization of small intestinal submucosa for recombinant adeno-associated virus serotype 2 binding and transduction. *Biomaterials* 28, 2350–2357. <https://doi.org/10.1016/j.biomaterials.2007.01.035>.
 36. Moon, I.S., Berglundh, T., Abrahamsson, I., Linder, E., and Lindhe, J. (1999). The barrier between the keratinized mucosa and the dental implant. An experimental study in the dog. *J. Clin. Periodontol.* 26, 658–663. <https://doi.org/10.1034/j.1600-051x.1999.261005.x>.
 37. Ma, S., Xu, S., Li, M., Du, Y., Tian, G., Deng, Y., Zhang, W., Wei, P., Zhao, B., Zhang, X., et al. (2023). A Bone Targeting Nanoparticle Loaded OGP to Restore Bone Homeostasis for Osteoporosis Therapy. *Adv. Healthc. Mater.* 12, e2300560. <https://doi.org/10.1002/adhm.202300560>.
 38. Allen, A.B., Priddy, L.B., Li, M.T.A., and Guldberg, R.E. (2015). Functional augmentation of naturally-derived materials for tissue regeneration. *Ann. Biomed. Eng.* 43, 555–567. <https://doi.org/10.1007/s10439-014-1192-4>.
 39. McDevitt, C.A., Wildey, G.M., and Cutrone, R.M. (2003). Transforming growth factor-beta 1 in a sterilized tissue derived from the pig small intestine submucosa. *J. Biomed. Mater. Res. A* 67, 637–640. <https://doi.org/10.1002/jbm.a.10144>.
 40. Voytik-Harbin, S.L., Brightman, A.O., Kraine, M.R., Waisner, B., and Badylak, S.F. (1997). Identification of extractable growth factors from small intestinal submucosa. *J. Cell. Biochem.* 67, 478–491.
 41. Xiaojie, W., Banda, J., Qi, H., Chang, A.K., Bwalya, C., Chao, L., and Li, X. (2022). Scarless wound healing: Current insights from the perspectives of TGF- β , KGF-1, and KGF-2. *Cytokine Growth Factor Rev.* 66, 26–37. <https://doi.org/10.1016/j.cytogfr.2022.03.001>.
 42. Oudhoff, M.J., Bolscher, J.G.M., Nazmi, K., Kalay, H., van 't Hof, W., Amerongen, A.V.N., and Veerman, E.C.I. (2008). Histatins are the major wound-closure stimulating factors in human saliva as identified in a cell culture assay. *FASEB J.* 22, 3805–3812. <https://doi.org/10.1096/fj.08-112003>.
 43. Ridley, A.J., Schwartz, M.A., Burridge, K., Firtel, R.A., Ginsberg, M.H., Borisy, G., Parsons, J.T., and Horwitz, A.R. (2003). Cell migration: integrating signals from front to back. *Science* 302, 1704–1709. <https://doi.org/10.1126/science.1092053>.
 44. Berditchevski, F. (2001). Complexes of tetraspanins with integrins: more than meets the eye. *J. Cell Sci.* 114, 4143–4151. <https://doi.org/10.1242/jcs.114.23.4143>.
 45. Longmate, W.M., and Dipersio, C.M. (2014). Integrin Regulation of Epidermal Functions in Wounds. *Adv. Wound Care* 3, 229–246. <https://doi.org/10.1089/wound.2013.0516>.
 46. Schwarz, F., Mihatovic, I., Golubovic, V., Bradu, S., Sager, M., and Becker, J. (2015). Impact of plaque accumulation on the osseointegration of titanium-zirconium alloy and titanium implants. A histological and immunohistochemical analysis. *Clin. Oral Implants Res.* 26, 1281–1287. <https://doi.org/10.1111/clr.12452>.
 47. Cai, R., Liu, Y., Wang, X., Wei, H., Wang, J., Cao, Y., Lei, J., and Li, D. (2023). Influences of standardized clinical probing on peri-implant soft tissue seal in a situation of peri-implant mucositis: A histomorphometric study in dogs. *J. Periodontol.* 21, 46. <https://doi.org/10.1002/jper.23-0167>.
 48. Salonen, J.I., Kautsky, M.B., and Dale, B.A. (1989). Changes in cell phenotype during regeneration of junctional epithelium of human gingiva *in vitro*. *J. Periodontol. Res.* 24, 370–377. <https://doi.org/10.1111/j.1600-0765.1989.tb00885.x>.
 49. Kim, A.S., Abdelhay, N., Levin, L., Walters, J.D., and Gibson, M.P. (2020). Antibiotic prophylaxis for implant placement: a systematic review of effects on reduction of implant failure. *Br. Dent. J.* 228, 943–951. <https://doi.org/10.1038/s41415-020-1649-9>.

50. Makkar, H., Atkuru, S., Tang, Y.L., Sethi, T., Lim, C.T., Tan, K.S., and Sriram, G. (2022). Differential immune responses of 3D gingival and periodontal connective tissue equivalents to microbial colonization. *J. Tissue Eng.* *13*. 20417314221111650. <https://doi.org/10.1177/20417314221111650>.
51. Jiang, Q., Yu, Y., Ruan, H., Luo, Y., and Guo, X. (2014). Morphological and functional characteristics of human gingival junctional epithelium. *BMC Oral Health* *14*, 30. <https://doi.org/10.1186/1472-6831-14-30>.
52. Kinumatsu, T., Hashimoto, S., Muramatsu, T., Sasaki, H., Jung, H.S., Yamada, S., and Shimono, M. (2009). Involvement of laminin and integrins in adhesion and migration of junctional epithelium cells. *J. Periodontol.* *Res.* *44*, 13–20. <https://doi.org/10.1111/j.1600-0765.2007.01036.x>.
53. Ma, S., Hu, H., Wu, J., Li, X., Ma, X., Zhao, Z., Liu, Z., Wu, C., Zhao, B., Wang, Y., and Jing, W. (2022). Functional extracellular matrix hydrogel modified with MSC-derived small extracellular vesicles for chronic wound healing. *Cell Prolif.* *55*, e13196. <https://doi.org/10.1111/cpr.13196>.

STAR★METHODS

KEY RESOURCES TABLE

REAGENT or RESOURCE	SOURCE	IDENTIFIER
Chemicals, peptides, and recombinant proteins		
Histatin1	Jill Biochemical Co., Ltd.	N/A
1-Ethyl-3-(3-dimethyl aminopropyl)carbodiimide (EDC)	Solarbio	CAS:25952-53-8
N-hydroxy succinimide (NHS)	Solarbio	CAS:35013-72-0
LIVE/DEAD® Cell Imaging Kit	Sigma	04511-1KT-F
Cell counting Kit-8 (CCK-8)	Solarbio	Cat# C0039
4',6-Diamidino-2-phenylindole, dihydrochloride(DAPI)	Solarbio	CAS:28718-90-3
Hematoxylin and Eosin Staining Kit	Solarbio	Cat:G1120
Rhodamine B	Solarbio	CAS:81-88-9
Oligonucleotides		
Primers for qRT-PCR, see Table S1	This paper	N/A
Software and algorithms		
Image J	NIH	https://imagej.nih.gov/ij/download.html
GraphPad Prism	GraphPad	https://www.graphpad.com/

RESOURCE AVAILABILITY

Lead contact

Further information and requests for resources and reagents should be directed to and will be fulfilled by the lead contact, Yonglan Wang (tmuperiodontology@163.com).

Materials availability

All materials are from commercial sources and are widely available.

Data and code availability

Original data are available from corresponding authors.

This paper does not report the original code.

Any additional information required to reanalyze the data reported in this paper is available from the [lead contact](#) upon request.

EXPERIMENTAL MODEL AND SUBJECT DETAILS

Cell lines

Human oral mucosa was taken out under aseptic conditions, washed twice with PBS solution containing double antibodies and soaked for 5 minutes. The tissue was cut into 0.5mm³, rinsed twice with PBS solution, centrifuged at 1000r/3min for 3 minutes, and the precipitate was collected. The tissue was resuspended with mixed collagenase and digested at 4°C overnight. Complete medium of human oral epithelial cells was added to terminate digestion. Filter the digestive suspension and tissue with 200 mesh sterile nylon net, collect the suspension, and centrifuge at 1000r/5min for 5 minutes.

METHOD DETAILS

Preparation of hydrogels

Fresh pig small intestine was washed, and the serosal layer and muscular layer were mechanically removed to obtain the original SIS. Degreasing, enzymoly SIS, digestion, washing, SIS -80°C in a freeze dryer (GAMMA 2-16 LSC; Christ, Germany), and then freeze-dried in a frozen mill (MM400; Retsch, German). The obtained SIS powder was stirred in an aqueous solution containing 3% acetic acid and 0.1% pepsin (25°C) for 48h, and the obtained SIS digestive solution was lyophilized again to obtain a soluble SIS matrix, which was sterilized with ethylene oxide gas. Add 50mM EDC and 50mM NHS into Hst1 solution (10μg, 100μg) and SIS (10 ml) matrix, stir for 6h, and dialyze in the dark for 24h. Then, 2.5 M NaOH was added to neutralize to pH 7.4, and the neutralized solution formed gel at 37°C. (Hst1 was manufactured by Jill biochemical co., ltd. (Shanghai, China). Finally, the scaffold was rinsed four times with PBS and DMEM.⁵³

Characterizations

Morphology

The hydrogel was freeze-dried at -80°C in a freeze-dryer (Gamma 2–16 LSC, Christ, Germany) for 24h. After the freeze-dried sample was added to the gold scanning electron conductive layer, the surface and cross-section of the material were observed. The microscopic image was obtained by scanning electron microscope (SEM, Gemini 300; Zeiss, Germany). The sol-gel transition behavior was observed by the vial tilt method. SIS-Hst1 was added into the vial and incubated at 37°C to observe the fluidity in real-time.

Release of hst1 in vitro

The hydrogel formed by FITC-Hst1 was used to simulate the release of Hst1 and incubated stably at 37°C and 100 rpm in an oscillating water bath. Soak the gel in PBS, collect 1ml of the released solution every day, and replace it with fresh PBS of equal volume. The absorbance was measured by ultraviolet spectrophotometer (BIOTEK)480 nm, and the release amount was calculated. The standard curve was measured by gradient dilution of FITC-Hst1 in PBS.

Rheology

HR-2 rheometer (AR-G2; TA Instrument, USA) to measure the rheological properties of the hydrogel. The storage modulus (G') of SIS and SIS-Hst1 hydrogels was monitored at 37°C with 1% stress-strain and 1hz frequency over time. At constant angular frequency (10 rad s^{-1}), the storage modulus (G') and loss modulus (G'') of hydrogels were measured by strain amplitude scanning (0.1% -1000%). In addition, the compression test of hydrogel was carried out at 37°C using the load cell of PC compressor (Minnesota, USA). The cylindrical hydrogel ($\phi 10\text{ mm} \times 5\text{ mm}$) on the lower plate was compressed at a compression rate of 5 mm/min to obtain the stress-strain curve.

Degradation

To determine the degradation, the hydrogel was placed in PBS containing collagenase (Sigma). Accurately weigh 1ml of hydrogel with the same mass, weigh the sample mass (W_0) after freeze-drying, soak it in 15 ml of enzyme buffer at 37°C for degradation, continuously weigh the remaining hydrogel mass (W_t) every day, and stop the degradation after 2 weeks. The calculation formula of degradation degree: degradation degree (%) = $(1 - W_t/W_0) \times 100$.

Swelling properties

Weigh a certain amount of hydrogel into artificial saliva, placing it in a wat bath at 37°C , taking out that hydrogel at regular intervals, wiping the surface moisture with wet filter paper, weighing it, then putting it back into the solution, and calculating the swelling ratio according to the quality before and after swelling at different time points. The formula for calculating the swelling ratio (Q) is: $Q = (m_t - m_0) / m_0$ (m_t is the mass of hydrogel when the swelling time is t , and m_0 is the initial gel.).

Antioxidant experiment

Cell live/dead staining

To evaluate the hGECs cell compatibility, take 100 μl of the hydrogel and put it in a 24-well plate. The control group was blank. After incubation for 12/24h, cells in 24-well plates were stained with live/dead reagents for 20 minutes, and images were obtained by inverted fluorescence microscope (Olympus IX71, Japa). Take photos in any five fields of vision, and count the number of cells in the microscope field of vision by ImageJ.

CCK-8 experiment

To evaluate cell proliferation, 10 μl of solidified gel was placed in a 96-well plate, and 5×10^3 cells were inoculated in each well with titanium plate culture medium without fetal bovine serum (the control group was blank). On Days 1, 3, 5, and 7, LDH levels in cell supernatants were measured using a Lactate dehydrogenase kit (LDH kit; Solarbio), and absorbance (OD) at 450 nm was measured using a microplate reader (Multiskan FC, USA) to determine the relative cell viability.

Antibacterial test

Inhibition zone experiment

Hydrogel were prepared using a fixed-size circular die, 100 μL of 106 cfu/mL *S. gordonii* bacterial solution was inoculated on BHI agar plates and incubated for 30 minutes at 37°C . After bacterial colonization, 100–1000 μL pipette was used to drill holes in the agar plate. Three groups of hydrogel prepared in advance were placed in the hole, and PBS was added as the blank control. Culture in an incubator at 37°C for 24 hours.

Live/dead staining

Hydrogel (1mL) were immersed in each contain 2mL of *S. gordonii* and incubated at 37°C for 12 h. The bacterial solution (100 μL) was then removed from the tube and stained with a live/dead staining kit. Bacterial suspensions in sterile PBS were used as controls. Live bacteria (green) and dead bacteria (red) were observed with CLSM.

Bacterial growth plate

Each 20 μ L suspension of *S. gordonii* were added on the surface of hydrogel for 12 h. Bacterial suspension (20 μ L) in sterile PBS (1 mL) was used as control. Add sterile PBS diluted bacterial suspension to each well, and spread the diluted bacterial suspension (10 μ L) evenly on BHI agar plate. After 24 h, photos were taken and the number of colony forming units (CFU) was calculated.

Cell adhesion and migration

Cell adhesion

Human gingival epithelial cells (hGECs) were resuspended in serum-free medium, and the density of cell suspension was adjusted to 1×10^6 cells/ml. 100 μ L of epithelial cell suspension was placed in the upper chamber of TRANSWELL. Hydrogel, DMEM, and 10% FBS were added to the orifice plate of the lower chamber (the control group was DMEM and 10% FBS). After 24h, the migrated cells were collected from the lower chamber, stained with crystal violet, and observed under a microscope. After that, the visual field was randomly selected and counted by ImageJ.

Cytoskeleton and cell morphology

To observe cell morphology, after each group was cultured on a titanium plate for 24h, the hGECs cultured on the samples were fixed with 4% paraformaldehyde and dehydrated in a gradient manner in an ethanol solution (30%, 50%, 75%, 90%, 95%, and 100%). SEM photographed the cell morphology on the titanium surface.

After 12h of culture, cytoskeletal actin was stained. The cells were fixed at 4°C with 4% paraformaldehyde, infiltrated with 0.25% Triton X-100 (Solarbio), and protected from light. The nuclei were stained with DAPI (Thermo-Fisher Scientific) and actin rhodamine B (Thermo Fisher Scientific). Photographs were taken by confocal laser scanning microscopy (CLSM; Zeiss, Baden-Württemberg, Germany).

Real-time quantitative polymerase chain reaction (qRT-PCR)

Cells were inoculated into six-well plates with or without gel, and the control group was the blank group. Extract the cell suspension, extract the RNA by TRIzol, then add an appropriate amount of enzyme-free (DEPC) water to dissolve the RNA, and measure the RNA concentration. The reaction system of GoScript reverse transcription was formulated, reverse transcription was performed at 50°C, and inactivated at 85°C. The cDNA was obtained, and qRT-PCR was performed by the Roche LC480II system (Roche, Switzerland). Results were calculated using the $\Delta\Delta C_t$ method. GAPDH is the control, and the primers are shown in table .

Western blot

The expression levels of laminin 5, integrin- $\alpha 6$, and integrin- $\beta 4$ and protein in the cells were detected by Western Blot. After the protein samples were prepared, the total protein content was determined by Bradford kit. The samples were subjected to concentration adjustment, SDS-PAGE electrophoresis, transfer, blocking, and incubation at 4°C with 1: 1000 primary antibody (Abcam, UK) and the corresponding 1: 5000 secondary antibody (Abcam, UK). Finally, the protein was detected using an ECL western blot substrate (Thermo Fisher Scientific, USA). Quantitative analysis was performed using ImageJ and the relative expression levels of laminin 5, integrin- $\alpha 6$, and integrin- $\beta 4$ proteins were normalized to GAPDH.

Immunofluorescence staining

Cells were inoculated into 24 well plates with or without gel, and the control group was the blank group. Fixed in 4% formaldehyde with 0.5% (v/v) Triton X-100 permeation. 5 mg/ml BSA solution was blocked and mixed with the primary antibody (Abcam, UK) and incubated overnight. Operate in the dark, and the secondary antibody (Abcam, UK) was incubated at 37°C for 2h. The nuclei were stained with a DAPI (Abcam, UK). The stained cells were observed and analyzed for the location and expression of laminin 5, In- $\alpha 6$, and In- $\beta 4$ in hGECs using CLSM. The nuclei were stained with a DAPI solution. Stained cells were observed and analyzed using CLSM for localization and expression of laminin 5, integrin- $\alpha 6$, and integrin- $\beta 4$ in hGECs.

Animal experiments in vitro

The animal experiment has been approved by Tianjin Medical University Animal Ethics Committee. According to the above experiment, the SIS-Hst1(H) group was selected as the experimental group. Eight-week-old SD rats were anesthetized by inhalation combined with intraperitoneal anesthesia, and the right upper first molar was extracted. The rats were randomly divided into three groups: blank implant, SIS hydrogel, and SIS-Hst1 hydrogel. The hydrogel was implanted with the implant. The drug was administered once every two days. After 1 week, the gingival specimens at the junction of implant and epithelium were obtained and stained with HE and immunofluorescence. Stained sections were visualized by NDP. View 2INC software after shooting with Vectra Polarix (PerkinElmer, USA).

QUANTIFICATION AND STATISTICAL ANALYSIS

All experiments in this study contain at least 3 repeated samples ($n \geq 3$), and all the experiments are repeated more than 3 times. One-way ANOVA and independent sample t test were used to analyze the data of each group, and the variables were expressed by the average standard deviation (SD). $p < 0.05$ was statistically significant.